Research Article Vol. 30, No. 3 / 31 Jan 2022 / Optics Express 4165
Optics EXPRESS

Scattering of partially coherent vortex beam by rough surface in atmospheric turbulence

KANGJUN DONG,[1,2] MINGJIAN CHENG,[1,4] MARTIN P. J. LAVERY,[3] SIQI GENG,[1] PING WANG,[1] AND LIXIN GUO[1,*]

[1] School of Physics and Optoelectronic Engineering, Xidian University, Xi'an 710071, China
[2] School of Physics and Electronic Engineering, Weinan Normal University, Weinan 714099, China
[3] School of Engineering, University of Glasgow, Glasgow G12 8LT, UK
[4] mjcheng@xidian.edu.cn
[*] lxguo@xidian.edu.cn

Abstract: A double-passage propagation model of partially coherent Laguerre-Gaussian (LG) vortex beams with orbital angular momentum (OAM) modes in turbulent atmosphere after scattering from Gaussian rough surfaces was formulated. Rough surface scattering had a weak effect on the spreading of a vortex beam in turbulent atmosphere. However, it severely influenced the phase on this beam, rapidly reducing the original OAM mode's relative intensity. The OAM spectrum information is more useful than the intensity information for rough surface object remote sensing. Additionally, by comparing the scattering intensity in monostatic and bistatic systems, the enhanced backscatter of vortex beams from Gaussian rough surfaces was verified.

1. Introduction

Spatially structured light, such as vortex beams, can carry both spin angular momentum (SAM) associated with polarization and orbital angular momentum (OAM) lined to a helical-shaped phase wavefront [1,2]. Vortex beam OAM modes can provide an infinite basis set for free-space optical (FSO) communication links, which have drawn considerable attention as a promising technology to increase channel capacity without increasing the spectral bandwidth [3,4]. However, for OAM-based FSO communication systems operated in the turbulence channel, fluctuations in refractive indexes along the transmission path can severely distort the vortex beam phase leading to the cross-coupling between signal modes and channel crosstalk [5]. Due to the effect of turbulent disturbance, the stability and reliability of OAM-based communication links sharply decrease with the increase in the mode number of transmitted OAM, thereby limiting the application of OAM modes to optical communication fields. In contrast, Lavery et al. [6] demonstrated that a frequency shift was proportional to the product of object rotation frequency and OAM mode when the vortex beam was scattered from a spinning object. Since then, target recognition based on the vortex beam has attracted considerable attention due to its ability to detect an object's characteristic information by exploiting the OAM data of vortex beams scattered from the object [7]. The development of target recognition applications using vortex beams requires fundamentally understanding the interaction mechanism of OAM modes with various objects. The generalized Lorenz-Mie theory [8] was widely used to solve the scattering problem of spherical or coated-spherical particle illuminated by various vortex beams [9–12]. Studies showed that the scattering properties of vortex beams were more sensitive to changes in the characteristic parameters of particles compared with those of plane and Gaussian beams. Furthermore, the finite-difference time-domain method [13], multilevel fast multipole algorithm [14], and method of moments [15] algorithms were applied to investigate the scattering of arbitrary shaped particles illuminated by vortex beams. Overall, vortex beams with OAM modes have been shown as more advantageous than Gaussian beams on acquiring target feature parameters.

#444155 https://doi.org/10.1364/OE.444155
Journal © 2022 Received 18 Oct 2021; revised 13 Jan 2022; accepted 15 Jan 2022; published 25 Jan 2022

Optics EXPRESS

The double passage of light beams through the atmospheric turbulence channel to a target and back through exactly the same atmospheric turbulence in the opposite direction (i.e., monostatic turbulence) can enhance the mean irradiance near the optical axis; this is known as enhanced backscatter [16]. The statistical average and instantaneous echo speckle characteristics of the double passage of vortex beams through monostatic turbulence via a retroreflector were experimentally measured in [17]. When mainly concerned the coherence scattering characteristics, those materials that have homogeneous isotropically rough surfaces and homogeneous subsurface scattering properties, for laser incidence can be considered equivalent to random rough surfaces in which the surface roughness correlation length is in terms of wavelength, [18,19]. For remote sensing and recognition based on vortex beams, research on enhanced backscatter and related double-passage problems of vortex beams scattered by rough surfaces in atmospheric turbulence is essential. The echo speckle characteristics of Laguerre-Gaussian (LG) vortex beams scattered from random rough surfaces were examined in [20] based on the Rytov approximation theory. The investigation showed that the atmospheric turbulence on coherence lengths and the scintillation effects of vortex beam echoes were observed to be less than those of Gaussian beams. Compared with the Rytov approximation theory, the multi-phase screen propagation method can derive the statistical average and instantaneous transmission characteristics [21,22]. Hence, it is a more efficient numerical method for simulating vortex beam propagation through the atmospheric turbulent channel. Moreover, fully coherent beams are extremely sensitive to atmospheric turbulence. In contrast, partially coherent beams are more resistant to the deleterious effects of turbulence than fully coherent beams [23]; thus, it can perform a robust function when used in FSO communication links and target recognition application. Such facts motivated us to study the double-passage and OAM characteristics of partially coherent vortex beams scattered by random rough surface in atmospheric turbulence. To this end, the theory of multi-phase screen propagation is introduced to describe the double-passage propagation of partially coherent LG vortex beam and spiral spectrum expansion method is employed to solve the OAM spectrum distribution problems of vortex beam echo in turbulent atmospheric channels.

The paper is organized as follows. In Section 2, the theoretical model of the double-passage propagation of partially coherent LG vortex beams in turbulent atmosphere is established based on multi-phase screen propagation theory, and the light intensity and phase distribution, beam spreading, OAM spectrum, and EBS effect of the partially coherent vortex beams scattered by random Gaussian rough surfaces can be analyzed. Section 3 shows the numerical results of this work, and Section 4 gives a summary of the paper.

2. Numerical simulation model of partially coherent LG vortex beams in turbulent atmosphere

Assume that the incidence of a vortex beam on a random Gaussian rough surface at distance L from the transmitter is scattered backward and received in the plane of the transmitter, i.e., monostatic system, as shown in Fig. 1(a). The atmospheric turbulence channels before and after the random Gaussian rough surface are the same but in the opposite direction. In another case of a bistatic system, the transmitter and receiver are mounted on two separate platforms. Moreover, vortex beams propagate through the atmospheric turbulence to a random Gaussian rough surface target, and echo waves propagate back through the atmospheric turbulence of the same length. As shown in Fig. 1(b), atmospheric turbulence channels in the forward and backward paths of the bistatic system can be unfolded in the same direction. In the simulation of double-passage propagation, a partially coherent LG vortex beam $U(\rho, 0)$ is generated at the transmitter. After passing through the forward path of atmospheric turbulence at a distance L and reflected from the rough surface target, the incident field is transformed into a scattered field. As the echo wave arrives at the receiver through the backward path of atmospheric turbulence at a distance L, the final scattered field of partially coherent LG vortex beams at the receiver can be obtained.

Optics EXPRESS

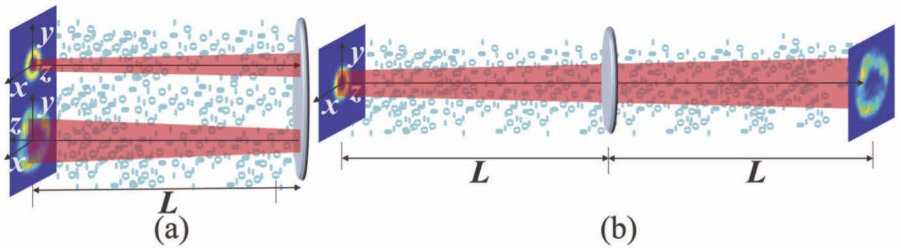

Fig. 1. Model of a double-passage propagation of a laser beam. (**a**) Monostatic system. (**b**) Bistatic system.

In the laboratory, a partially coherent LG vortex beam can be generated by sending a fully coherent LG vortex beam through a rotating ground glass or a phase diffuser with a spatially random phase pattern. The rotational frequency of the ground glass or phase diffuser must be sufficiently high such that during the detection process, many realizations of the spatially random phase pattern are presented. Then, LG vortex beam is expected to appear with a partially coherent characteristic. Similarly, numerical simulation method for generating a partially coherent LG vortex beam from a fully coherent source requires a time average over many realizations of an applied random phase pattern that has a Gaussian correlation function. To accomplish this, a series of spatially random and time-varying phase modulated random screens is introduced into the fully coherent LG vortex beam [24]. The random phase modulation period must be shorter than the integration time of the distortion of atmospheric turbulence. According to the random phase screen theory, the field $U(x, y, t)$ of a partially coherent LG vortex beam at the source field after phase modulation can be expressed as follows:

$$U(x, y; t) = U_0(x, y)t(x, y; t), \tag{1}$$

where $t(x, y; t) = \exp[i\phi(x, y; t)]$ is the spatial modulation signal or transmittance, $\phi(x, y; t)$ represents the random phase characterized by the coherence of light field. $U_0(x, y)$ is the field of the initial fully coherent LG vortex beam before phase modulation,

$$E(r, \theta, 0) = \frac{1}{w_0}\sqrt{\frac{2p!}{\pi(p + |l|)!}}\exp\left(-\frac{r^2}{w_0^2}\right)L_p^{|l|}\left(\frac{2r^2}{w_0^2}\right)\left(\frac{\sqrt{2}r}{w_0}\right)^{|l|}\exp(-il\theta), \tag{2}$$

where l and p denote the OAM angular mode (topological charge) and radial mode of LG vortex beam, respectively. w_0 is the initial waist radius of beam, $L_p^{|l|}()$ is the Laguerre polynomials, r and θ represent the radial distance and azimuth angle, respectively. The complex correlation function of the spatially modulated signal usually can be expressed as follows and has a form of Gaussian function [16]:

$$R(x', y') = \langle t(x + x', y + y'; t) \cdot t^*(x, y; t)\rangle = \exp\left(-\frac{x'^2 + y'^2}{l_{cr}^2}\right), \tag{3}$$

where l_{cr} is the spatial coherence length and describes the partially coherence properties of the beam source. For a fully coherent beam, l_{cr} approaches to infinity, and the degree of source coherence declines with the decreasing l_{cr}.

Based on the convolution of a two-dimensional random Gaussian signal $r(x, y; t)$ and a Gaussian filter function $f(x, y)$, random phase $\phi(x, y; t)$ can be expressed as,

$$\phi(x, y) = r(x, y; t) \otimes f(x, y), \tag{4}$$

Optics EXPRESS

where $\otimes$ indicates a spatial convolution and Gaussian filter function $f(x, y)$ has the expression,

$$f(x,y) = \frac{1}{\pi\sigma_f^2}\exp\left(-\frac{x^2+y^2}{\sigma_f^2}\right). \tag{5}$$

Thus, the correlation function of random phase $\phi(x, y; t)$, i.e. Equation (3) can be obtained as:

$$R(x',y') = \exp\left\{-\frac{\sigma_r^2}{\pi\sigma_f^2}\left[1-\exp\left(-\frac{x'^2+y'^2}{\sigma_f^2}\right)\right]\right\}. \tag{6}$$

As $\frac{\sigma_r^2}{2\pi\sigma_f^2} \gg 1$, the formula Eq. (6) can be further simplified to:

$$R(x',y') = \exp\left(-\frac{x'^2+y'^2}{4\pi\sigma_f^4/\sigma_r^2}\right). \tag{7}$$

By comparing Eq. (3) and Eq. (7), the expression of the spatial coherence length of partially coherent beam can be written as:

$$l_{cr}^2 = \frac{4\pi\sigma_f^4}{\sigma_r^2}. \tag{8}$$

The simulation of a partially coherent LG vortex beam propagation through the atmospheric turbulence channel in both forward and backward paths are accomplished through the multi-phase screen method [5]. According to the multi-phase screen propagation theory, vacuum transmission and turbulence-induced phase disturbance are regarded as independent and simultaneously complete processes. Atmospheric turbulence can be simulated by a series of thin random phase screens that are equally spaced over a link that is being simulated, as illustrated in Fig. 2. Here, the Von Kármán turbulent spectrum is adopted to generate a series of random phase screens, and each screen has its own value of Fried parameter r_0, turbulence outer scale L_0, and inner scale l_0,

$$\Phi_n(\beta\kappa) = 0.033C_n^2\frac{\exp\left(-\kappa^2/\kappa_m^2\right)}{\left(\kappa^2+\kappa_0^2\right)^{11/6}}, \tag{9}$$

where κ_m=5.92/l_0 and κ_0=1/L_0.

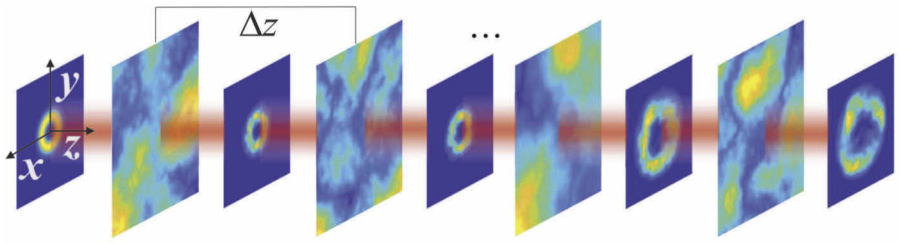

Fig. 2. Vortex beam propagation in atmospheric turbulence.

The simulation of a turbulent environment through layers of phase screens is modeled using the basic theory of phase screens. Each layer of phase screens represents a turbulent environment within the transmission distance of Δz. Its fundamental expression is:

$$U_1(x,y) = \mathrm{IFFT}\left\{\exp\left(i\kappa_z\Delta z\right)\mathrm{FFT}\left[U_0\left(x_0,y_0\right)\exp\left(iS\left(x_0,y_0\right)\right)\right]\right\}, \tag{10}$$

where $\kappa_z = \sqrt{\kappa^2-\kappa_x^2-\kappa_y^2}$, κ_x and κ_y are the spatial wave number of x and y drections, U_0 and U_1 represents the field intensity before and after turbulence phase screen. IFFT and FFT represent

Optics EXPRESS

the inverse Fourier transform and the Fourier transform. Turbulence-induced phase $S(x_0, y_0)$ is a Fourier-transformable function, we can write it in a Fourier-integral representation as

$$S(m'\Delta x, n'\Delta y) = \sqrt{\Delta\kappa_x \Delta\kappa_y} \sum_{m'=0}^{N-1} \sum_{n'=0}^{N-1} h\left(m''\Delta\kappa_x, n''\Delta\kappa_y\right) \sqrt{\Phi_n\left(m'\Delta\kappa_x, n'\Delta\kappa_y\right)} \times \exp\left[\frac{i2\pi}{N}(m'm'' + n'n'')\right] \tag{11}$$

where $\Delta\kappa_x$ and $\Delta\kappa_y$ are the frequency interval of x and y drections, Δx and Δy are grid spacing in two directions, $h\left(m''\Delta\kappa_x, n''\Delta\kappa_y\right)$ is random array which obey complex circular Gaussian statistics with zero-mean and unit-variance; N is the gird number of phase screen, m', n', m'' and n'' are the integer indices.

If the partially coherent random phase modulation is changed through K times realizations, and time averaging is applied, then parameter K (during the period in which the atmospheric turbulence changes only once) is named as the relative change frequency. After propagating K times through the same atmospheric turbulence channel, the resulting light beam irradiance profile exhibits partially coherent characteristics that are related to the spatial correlation function of applied phase modulation. The numerical simulation and statistical process of partially coherent LG vortex beams propagation through the turbulent atmospheric channel in this study are as follows:

(1) the multi-phase screen method based on spectrum inversion is employed to generate a series of atmospheric turbulent random phase screens with the same interval of Δz along the transmission path with a total distance of L;

(2) K partially coherent random phase screens are produced and superimposed on a fully coherent LG vortex beam to obtain K frames of partially coherent LG vortex beam, and each frame of this beam is allowed to pass through $L/\Delta z$ random phase screens of atmospheric turbulence along the propagation path to obtain the irradiance distribution at each phase screen position;

(3) the irradiance distributions of K frames at each turbulent phase screen position are statistically averaged, thus developing the simulation model of K frames of partially coherent LG vortex beams propagating through the turbulent atmosphere;

(4) repeat the above steps m times, and obtain the statistical average of results of K frames of partially coherent LG vortex beam propagating through the turbulent atmosphere, thus enabling the analysis of the turbulent atmospheric effects on the partially coherent LG vortex beams.

Figure 3 shows the schematic of the above process.

When it comes to the target scattering problem, homogeneous and isotropically rough materials are considered in this investigation, the specification of partially coherent LG vortex beam incidence, rough materials can be considered equivalent to random rough surfaces, and a large number of materials possess these properties, rough surfaces are usually simplified into random phase screens during numerical simulation. There are two important parameters to describe the roughness of a rough surface: root mean square of height fluctuations σ_h and surface correlation length ρ_h. The height fluctuation power density spectrum of Gaussian rough surface can be expressed as [16]:

$$\Phi_h(\kappa) = \sqrt{\pi}\sigma_h^2 \exp(-\kappa^2\rho_h^2/4). \tag{12}$$

Using the power spectrum inversion method, the rough surface height distribution $h(\rho)$ can be obtained. In the case of the perpendicular incidence, scattered field of random rough surface can

Optics EXPRESS

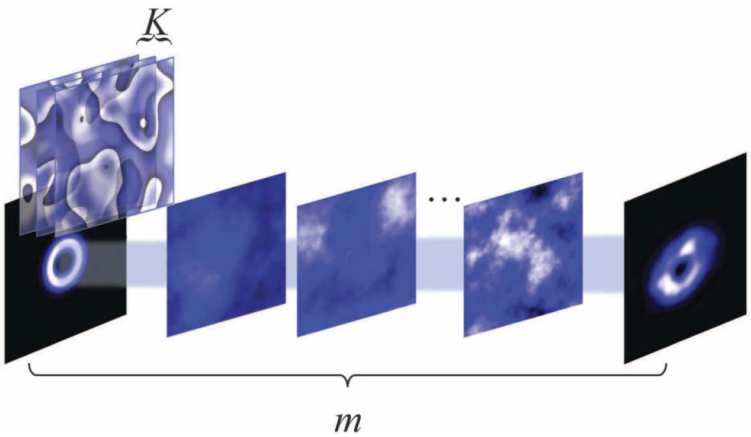

Fig. 3. Schematic of numerical process.

be approximately written as:

$$U_s(\rho) = R_d W(\rho) U(\rho) \exp[2ikh(\rho)], \tag{13}$$

where R_d is the reflectivity of rough surface, k is the wave number, $k = 2\pi/\lambda$, λ is the wavelength of light beam, and $W(\rho)$ is the aperture function, with the form as,

$$W(\rho) = \exp(-\rho^2/W_R^2), \tag{14}$$

where W_R is the target radius.

3. Results and discussion

In this section, to investigate the influence of atmospheric turbulence and Gaussian rough surface scattering on the propagation of partially coherent LG vortex beams and their OAM modes in a bistatic system, the intensity and phase distributions as well as the beam spreading and OAM spectrum of partially coherent LG vortex beams during double-passage atmospheric turbulence transmission are examined, the simulation parameters are summarized in Table 1, unless otherwise specified. Finally, the backscattering enhancement of partially coherent LG vortex beams in a monostatic system is analyzed.

Table 1. Parameter values in a double-passage propagation simulation of a partially coherent LG vortex beam in atmospheric turbulence.

Parameter	value	Parameter	value
Angular mode l	3	Radial mode p	0
Wavelength λ	633 nm	Waist radius w_0	0.04 m
Source spatial coherence length l_{cr}	0.02 m	Total distance $2L$	2000 m
Outer scale L_0	10 m	Inner scale l_0	0.001 m
Fried parameter r_0	0.01 m	Surface correlation length ρ_h	0.4 m
Root mean square of height fluctuations σ_h	$\sqrt{0.01\lambda}$	Target radius W_R	0.05 m
Relative change frequency K	10	Statistics times m	200
Reflectivity of rough surface R_d	1	Screen width d	0.2 m
Grid width N	512	Screen spacing Δz	50 m

Optics EXPRESS

3.1. Intensity and phase distributions

Based on the double-passage propagation model of partially coherent LG vortex beams in the turbulent atmosphere, Fig. 4 shows the intensity and phase distributions of partially coherent LG vortex beams before and after the beam is reflected by random Gaussian rough surfaces of different surface correlation lengths ρ_h and root mean squares of height fluctuation σ_h in the turbulent atmosphere. Although the intensity and phase distributions of vortex beams before scattering are under the same condition, there exist slight differences between them because of the random theory (each layer of the turbulent phase screen with the same simulation parameters is generated randomly). The effects that come from the surface scattering can be evaluated via the comparison of the intensity and phase distributions before and after scattering. The intensity and phase distributions of vortex beams are observed to change after the beam is reflected by random Gaussian rough surfaces. Although rough surface scattering has some effect on the intensity amplitude of the beams, the intensity distribution only undergoes relatively minor changes. In comparison, the effect of Gaussian rough surface scattering on phase distribution is more evident: with increasing surface roughness, phase distortion, which rises with the decrease in surface correlation length ρ_h and increase in root mean square of height fluctuation σ_h, is enhanced.

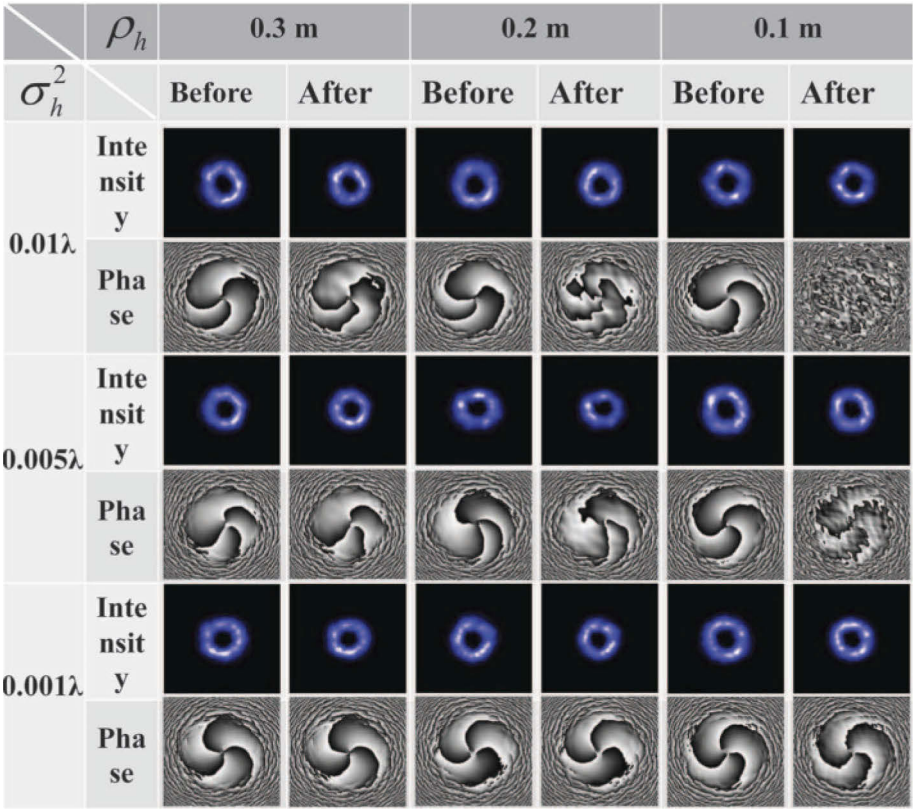

Fig. 4. Intensity and phase distribution diagrams of partially coherent LG vortex beams before and after reflected by random Gaussian rough surfaces of different surface correlation lengths and root mean squares of the height fluctuation in the turbulent atmosphere.

Optics EXPRESS

3.2. Beam spreading

To determine the beam width of partially coherent LG vortex beams in the atmospheric turbulence, an effective beam radius (spot size) ρ_r is introduced. In the range ρ_r, the energy accounts for $1 - \frac{1}{e^2}$ of the total energy of light beam in the space [16],

$$\frac{\int_0^{\rho_r} I(\rho)\, d\rho}{\int_0^{\infty} I(\rho)\, d\rho} = 1 - \frac{1}{e^2}. \tag{15}$$

For LG vortex beams, different OAM angular mode l and radial mode p correspond to different initial beam shapes and beam widths at the source plane. Making an accurate description of turbulence-induced beam spreading of partially coherent LG vortex beams with different topological charges in the atmosphere requires the relative beam spreading w_R, which is given by,

$$w_R = \frac{\rho_r(L)}{\rho_r(L=0)}. \tag{16}$$

The impact of topological charges l of partially coherent LG vortex beams on turbulence-induced beam spreading in the double-passage atmospheric channel is illustrated by changing the topological charges (i.e., l=1, 3, and 5), as shown in Fig. 5. The role of parameter topological charge l on the beam size of vortex beam is similar with beam size w_0, a vortex beam with larger topological charge l has a larger spot size in free space, and the larger spot size brings ensemble smoothing effect that can effectively weaken the turbulence induced beam spreading in the atmosphere. In the plane, at L = 1000 m, the effects of the same Gaussian rough surface scattering on the relative beam spreading of partially coherent LG vortex beams with different topological charge l values only slightly vary, as indicated by the virtual absence of mutation in the growth trends of the relative beam spreading.

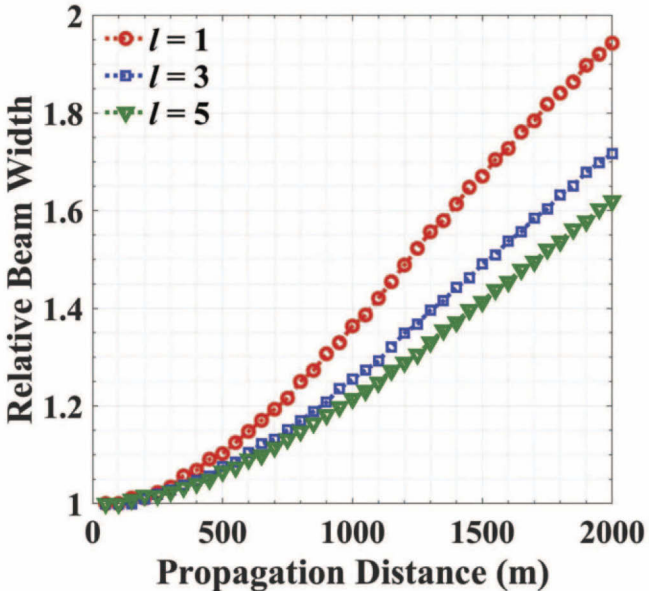

Fig. 5. Variations of relative beam spreading of partially coherent LG vortex beams with different topological charges l during double-passage atmospheric turbulence transmission.

The influence of random Gaussian rough surfaces with different root mean squares of height fluctuation σ_h on the relative beam spreading of partially coherent LG vortex beams during the

Optics EXPRESS

double-passage atmospheric turbulence transmission by changing σ_h^2 to 0.001λ, 0.005λ, and 0.01λ is presented in Fig. 6. As shown in the figure, after the beam is reflected by random Gaussian rough surfaces of different root mean squares of height fluctuation σ_h at $L = 1000$ m, the growth trend of the relative spreading of partially coherent LG vortex beams in the turbulent atmosphere changes. In particular, with increasing root mean square of height fluctuation σ_h, rough surface scattering becomes more violent, leading to the stronger relatively spreading of partially coherent LG vortex beams in the turbulent atmosphere.

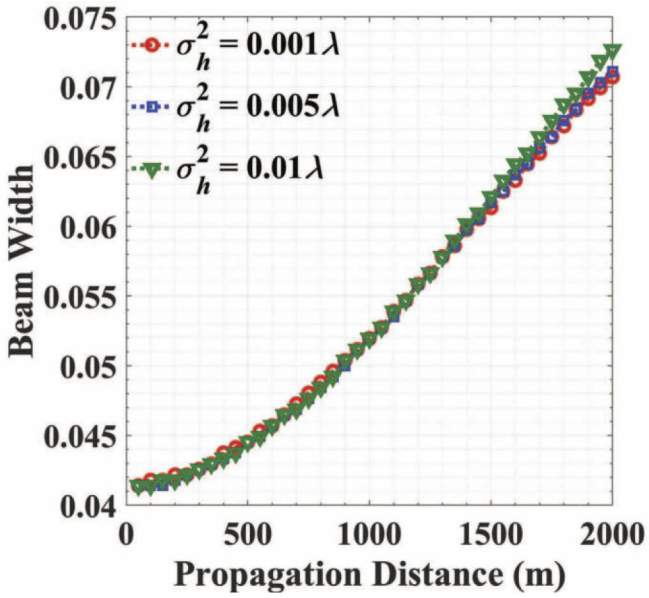

Fig. 6. Effects of the root mean square of height fluctuation on relative beam spreading of partially coherent LG vortex beams during double-passage atmospheric turbulence transmission.

The influence of random Gaussian rough surfaces with different surface correlation lengths (i.e., changing ρ_h to 0.2, 0.3, and 0.4 m) on the relative spreading of partially coherent LG vortex beams during double-passage atmospheric turbulence transmission is presented in Fig. 7. Consistent with the results shown in Fig. 7, the small value of the surface correlation length ρ_h of random Gaussian rough surfaces cause more drastic scattering, leading to the greater relative beam spreading of partially coherent LG vortex beams.

3.3. OAM spectral characteristics

During the double-passage atmospheric turbulence transmission process, the fluctuations in the refractive index lead to spatially varying phase delays that can sustainably alter the phase distribution of partially coherent LG vortex beams. The energy of the original OAM mode is assigned to its neighboring OAM modes. Based on the superposition theory of spiral harmonics, the energy redistribution scheme of the original OAM mode is developed to analyze the OAM spectral characteristics of partially coherent LG vortex beams during double-passage atmospheric turbulence transmission.

Expand the light field $E(x, y, z)$ of partially coherent LG vortex beams with spiral harmonic $\exp(il\theta)$, yields,

$$E(x, y, z) = \frac{1}{\sqrt{2\pi}} \sum_{l=-\infty}^{+\infty} a_l(r, z) \exp(il\theta). \tag{17}$$

Optics EXPRESS

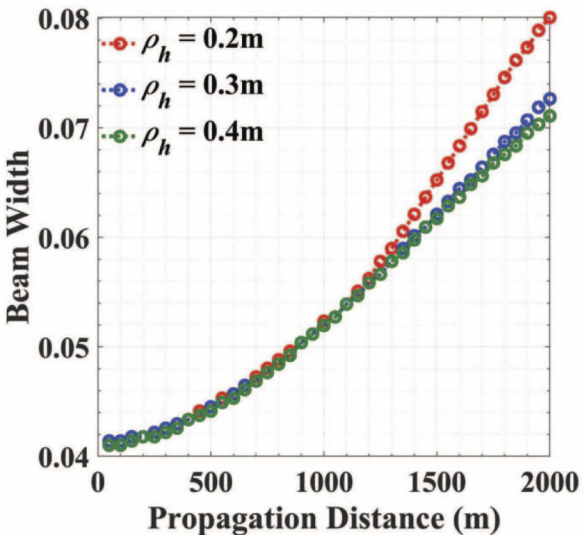

Fig. 7. Effects of surface correlation length on relative beam spreading of partially coherent LG vortex beams during double-passage atmospheric turbulence transmission.

where expansion coefficient a_l can be obtained by the following integral:

$$a_l(r,z) = \frac{1}{\sqrt{2\pi}} \int_0^{2\pi} E(x,y,z) \exp(-il\theta) d\theta. \tag{18}$$

The energy redistribution of the original OAM mode with quantum number l can be expressed as:

$$C_l = \int_0^{\infty} |a_l(r,z)|^2 r dr, \tag{19}$$

After the normalization of C_l, the relative intensity of the original OAM mode is given as:

$$R_l = \frac{C_l}{\sum_{q=-\infty}^{+\infty} C_q}. \tag{20}$$

Therefore, the OAM spectrum characteristics of partially coherent LG vortex beams during double-passage atmospheric turbulence transmission can be evaluated.

In Fig. 8, the OAM spectrum of partially coherent LG beams is plotted with different original OAM modes (i.e., $l = 1$, 3, and 5 at the receiver $2L$=2000 m) after the double-passage atmospheric turbulence transmission. The double-passage atmospheric turbulence channel clearly causes the crosstalk among OAM modes and induces the spread of the OAM spectrum of partially coherent LG beams. The effects of atmospheric turbulence on the OAM spectral characteristics of vortex beams aggravate with increasing original OAM mode quantum number l; this is consistent with the conclusion reached in the single-passage atmospheric turbulence transmission.

The impact of spatial coherence length l_{cr} on the OAM spectrum of partially coherent LG vortex beams at the receiver after the double-passage atmospheric turbulence transmission is also investigated, as shown in Fig. 9. To this end, the spatial coherence length l_{cr} is changed to 0.02, 0.04, and 0.06 m. Although atmospheric turbulence weakly affects the intensity fluctuation of partially coherent beams with a lower degree of source coherence, the spreading of the OAM spectrum of PCLGB increases with decreasing spatial coherence length l_{cr}. The OAM mode

Optics EXPRESS

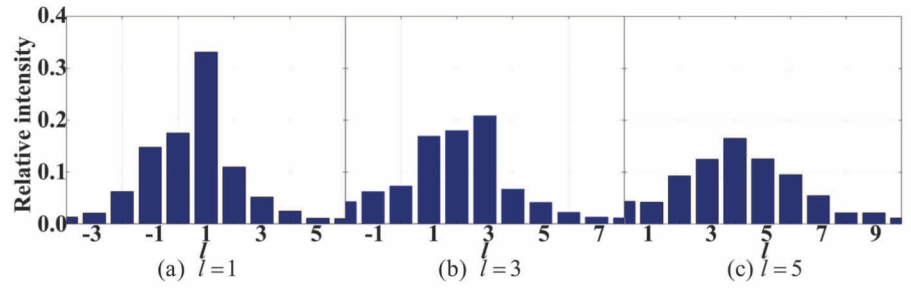

Fig. 8. Variations of OAM spectrum of partially coherent LG vortex beams with different topological charges l at the receiver after double-passage atmospheric turbulence transmission.

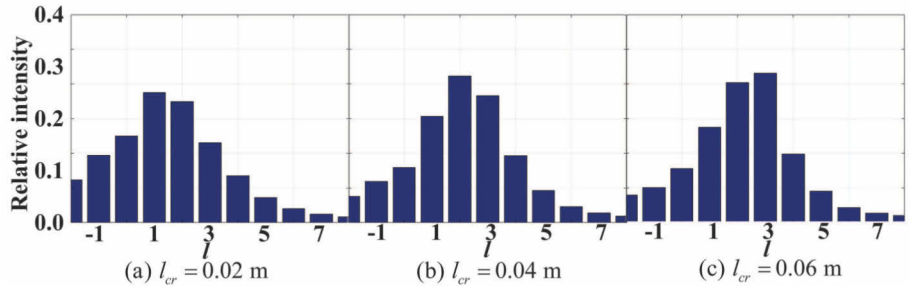

Fig. 9. Variations of OAM spectrum of partially coherent LG vortex beams with different spatial coherence lengths at the receiver after double-passage atmospheric turbulence transmission.

conveyed by the partially coherent LG vortex beams with a lower degree of source coherence is more affected by atmospheric turbulence.

The influence of random Gaussian rough surfaces with different root mean square of height fluctuation σ_h on the relative intensity of the original OAM mode conveyed by the partially coherent LG vortex beams during the double-passage atmospheric turbulence transmission is demonstrated in Fig. 10. Here, height fluctuation σ_h^2 is set to 0.001λ, 0.005λ, and 0.01λ. The transmission performance of OAM modes carried by vortex beam decrease with the propagation distance in the turbulence, reflected by the random Gaussian rough surface, the phase of vortex beam is further destroyed. Compared with Fig. 6, height fluctuation σ_h^2 of Gaussian rough surface has stronger effect on the relative intensity related with phase than the beam width related with intensity. The shape drops of the curve for $\sigma_h^2 = 0.01\lambda$ is reasonable, Gaussian rough surface scattering with larger height fluctuation σ_h^2 creates a stronger phase distortion on vortex beam, results in a drastic drop of the relative intensity of the original OAM mode during the double-passage atmospheric turbulence transmission.

The influence of coherence lengths ρ_h of random Gaussian rough surfaces on the relative intensity of the original OAM mode conveyed by the partially coherent LG vortex beams during the double-passage atmospheric turbulence transmission is illustrated by changing ρ_h (i.e., 0.2, 0.3, and 0.4 m), as shown in Fig. 11. It is indicated that random Gaussian rough surface scattering will cause the extra phase distortion on vortex beam, leading to the sharp drop of the relative intensity of the original OAM mode during the double-passage atmospheric turbulence transmission, and the amplitudes of variation increase with the increase of the height fluctuation σ_h^2 and the decrease of the surface coherence length ρ_h. After rough surface scattering, the relative intensity of the original OAM mode dropped and the OAM spectrum spreading enhanced.

Optics EXPRESS

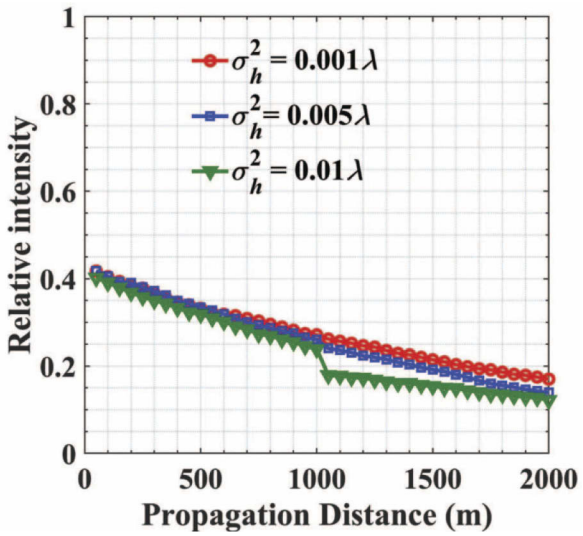

Fig. 10. Effects of root mean square of height fluctuation on relative intensity of the original OAM mode carried by partially coherent LG vortex beams during double-passage atmospheric turbulence transmission.

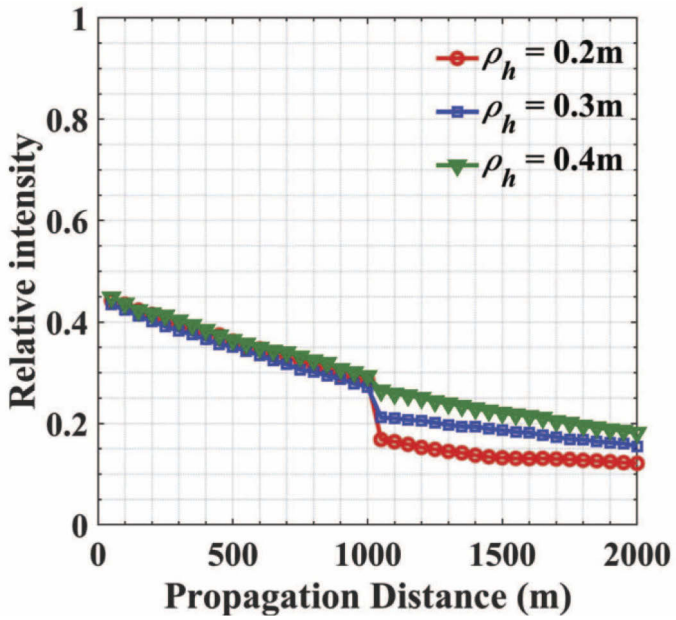

Fig. 11. Effects of surface correlation length on relative intensity of the original OAM mode carried by partially coherent LG vortex beams during double-passage atmospheric turbulence transmission

3.4. Backscattering enhancement

In the above bistatic systems, the atmospheric turbulence channels in the forward and backward paths are completely independent, and the atmospheric turbulence phase screens are randomly and independently generated during the simulation process. However, for monostatic systems,

Optics EXPRESS

atmospheric turbulence phase screens in the forward and backward paths must be consistently generated in the opposite direction. By comparing the partially coherent LG vortex beams propagation in monostatic and bistatic systems, the enhancement of atmospheric turbulence-induced backscattering is observed.

The intensity profiles of rough surface echo with the partially coherent LG vortex beams incidence in monostatic and bistatic systems at the receiver are shown in Fig. 12. The figure indicates that under the same calculation parameter conditions, the intensity profiles of rough surface echo in monostatic and bistatic systems basically coincide, except for a part in the optical axis. In the optical axis, the intensity amplitude of the echo in the monostatic system is slightly higher than that in the bistatic system. This phenomenon reveals that after the partially coherent LG vortex beams is reflected by the rough surface in the monostatic system, its echo also has a backward enhancement effect.

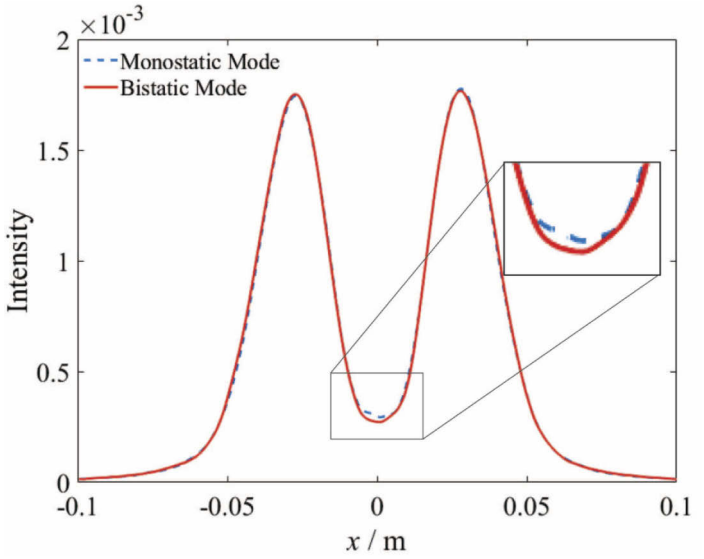

Fig. 12. Intensity profiles of rough surface echo with partially coherent LG vortex beams incidence in monostatic and bistatic systems at the receiver.

4. Conclusions

In this article, the effects of atmospheric turbulence and rough surface scattering on the propagation behavior of partially coherent LG vortex beams in the double-passage atmospheric turbulence channel were quantitatively described. Based on the phase screen theory, the double-passage propagation model of a partially coherent LG vortex beam reflected by random Gaussian rough surfaces in the turbulent atmosphere was formulated. It was also employed to analyze the intensity and phase distributions, beam spreading, OAM spectrum characteristics, and backscattering enhancement effects. The analysis results showed that random Gaussian rough surfaces had a minimal effect on the intensity pattern and beam spreading of partially coherent vortex beams in the atmospheric turbulence. In contrast, the phase distribution of a partially coherent LG vortex beam was more affected by rough surface scattering, resulting in a rapid descent of the relative intensity of the original OAM mode after the beam was reflected by rough surfaces. The remote sensing of random Gaussian rough surfaces by measuring the OAM spectral data was more effective than the traditional intensity pattern measurement method. The decreasing degree of source coherence aggravated the effects of atmospheric turbulence on the OAM spectral

Optics EXPRESS

characteristics of partially coherent LG vortex beams; this is consistent with the conclusion reached in the single-passage atmospheric turbulence transmission. By comparing the scattering intensity profiles of partially coherent LG vortex beams in monostatic and bistatic radar systems, the enhanced backscatter effects of vortex beams scattered from the Gaussian rough surface in the optical axis were distinctly observed.

Funding. National Natural Science Foundation of China (61621005, 61627901, 61901336, 61905186); Natural Science Foundation of Shaanxi Province (2020JQ-286).

Acknowledgments. The authors express their appreciation to the anonymous reviewers for their valuable suggestions.

Disclosures. The authors declare no conflicts of interest.

Data availability. No data were generated or analyzed in the presented research.

References

1. G. J. Gbur, *Singular optics* (CRC, 2016).
2. L. Allen, M. W. Beijersbergen, R. J. C. Spreeuw, and J. P. Woerdman, "Orbital angular momentum of light and the transformation of Laguerre-Gaussian laser modes," Phys. Rev. A **45**(11), 8185–8189 (1992).
3. J. Wang, J. Y. Yang, I. M. Fazal, N. Ahmed, Y. Yan, H. Huang, Y. Ren, Y. Yue, S. Dolinar, M. Tur, and A. E. Willner, "Terabit free-space data transmission employing orbital angular momentum multiplexing," Nat. Photonics **6**(7), 488–496 (2012).
4. A. E. Willner, H. Huang, Y. Yan, Y. Ren, N. Ahmed, G. Xie, C. Bao, L. Li, Y. Cao, and Z. Zhao, "Optical communications using orbital angular momentum beams," Adv. Opt. Photonics **7**(1), 66–106 (2015).
5. M. Chen and M. P. J. Lavery, *Optical angular momentum interaction with turbulent and scattering media, Structured Light for Optical Communication* (Elsevier, 2021).
6. M. P. J. Lavery, F. Speirits, S. Barnett, and M. Padgett, "Detection of a spinning object using light's orbital angular momentum," Science **341**(6145), 537–540 (2013).
7. L. Marrucci, "Spinning the Doppler effect," Science **341**(6145), 464–465 (2013).
8. G. Gouesbet, B. Maheu, and G. Grehan, "The order of approximation in a theory of the scattering of a Gaussian beam by a Mie scatter center," J. Opt. **16**(5), 239–247 (1985).
9. V. Garbin, G. Volpe, E. Ferrari, M. Versluis, D. Cojoc, and D. Petrov, "Mie scattering distinguishes the topological charge of an optical vortex: a homage to Gustav Mie," New J. Phys. **11**(1), 013046 (2009).
10. Y. Jiang, Y. Shao, X. Qu, J. Ou, and H. Hua, "Scattering of a focused Laguerre-Gaussian beam by a spheroidal particle," J. Opt. **14**(12), 125709–125716 (2012).
11. X. Zambrana-Puyalto and G. Molina-Terriza, "The role of the angular momentum of light in Mie scattering. Excitation of dielectric spheres with Laguerre–Gaussian modes," J. Quant. Spectrosc. Radiat. Transfer **126**(5), 50–55 (2013).
12. T. Qu, Z. Wu, Q. Shang, and J. Li, "Light scattering of a Laguerre–Gaussian vortex beam by a chiral sphere," J. Opt. Soc. Am. A **33**(4), 475–482 (2016).
13. M. Yang, Y. Wu, K. Ren, and X. Sheng, "Computation of radiation pressure force exerted on arbitrary shaped homogeneous particles by high-order Bessel vortex beams using MLFMA," Opt. Express **24**(24), 27979–27992 (2016).
14. W. Sun, Y. Hu, C. Weimer, K. Ayers, R. Baize, and T. Lee, "A FDTD solution of scattering of laser beam with orbital angular momentum by dielectric particles: Far-field characteristics," J. Quant. Spectrosc. Radiat. Transfer **188**, 200–213 (2017).
15. Z. Cui, S. Guo, J. Wang, F. Wu, and Y. Han, "Light scattering of Laguerre–Gaussian vortex beams by arbitrarily shaped chiral particles," J. Opt. Soc. Am. A **38**(8), 1214–1223 (2021).
16. L. C. Andrews and R. L. Phillips, *Laser beam propagation through random media* (SPIE, 2005).
17. J. Yu, Y. Huang, G. Gbur, F. Wang, and Y. Cai, "Enhanced backscatter of vortex beams in double-pass optical links with atmospheric turbulence," J. Quant. Spectrosc. Radiat. Transfer **228**, 1–10 (2019).
18. J. Leader, "An analysis of the frequency spectrum of laser light scattered from moving rough objects," J. Opt. Soc. Am. A **67**(8), 1091–1098 (1977).
19. J. Leader, "Analysis and prediction of laser scattering from rough surface materials," J. Opt. Soc. Am. A **69**(4), 610–629 (1979).
20. Y. Li, L. Wang, L. Gong, and Q. Wang, "Speckle characteristics of vortex beams scattered from rough targets in turbulent atmosphere," J. Quant. Spectrosc. Radiat. Transfer **257**, 107342 (2020).
21. B. Rodenburg, M. Mirhosseini, M. Malik, O. Maga na-Loaiza, M. Yanakas, L. Maher, N. Steinhoff, G. Tyler, and R. Boyd, "Simulating thick atmospheric turbulence in the lab with application to orbital angular momentum communication," New J. Phys. **16**(3), 033020 (2014).
22. M. P. J. Lavery, "Vortex instability in turbulent free-space propagation," New J. Phys. **20**(4), 043023 (2018).
23. D. Van and T. Visser, "Evolution of singularities in a partially coherent vortex beam," J. Opt. Soc. Am. A **26**(4), 741–744 (2009).
24. X. Xiao and D. Voelz, "Wave optics simulation approach for partial spatially coherent beams," Opt. Express **14**(16), 6986–6992 (2006).